Nonlinear Quantum Optics with Trion Polaritons in 2D Monolayers: Conventional and Unconventional Photon Blockade

O. Kyriienko,[1] D. N. Krizhanovskii,[2,3] and I. A. Shelykh[4,3]
[1]*Department of Physics and Astronomy, University of Exeter, Stocker Road, Exeter EX4 4QL, United Kingdom*
[2]*Department of Physics and Astronomy, The University of Sheffield, Sheffield S3 7RH, United Kingdom*
[3]*Department of Physics and Engineering, ITMO University, St. Petersburg 197101, Russia*
[4]*Science Institute, University of Iceland, Dunhagi-3, IS-107 Reykjavik, Iceland*

(Received 4 December 2019; accepted 24 September 2020; published 5 November 2020)

We study a 2D system of trion polaritons at the quantum level and demonstrate that for monolayer semiconductors they can exhibit a strongly nonlinear optical response. The effect is due to the composite nature of trion-based excitations resulting in their nontrivial quantum statistical properties, and enhanced phase space filling effects. We present the full quantum theory to describe the statistics of trion polaritons, and demonstrate that the associated nonlinearity persists at the level of few quanta, where two qualitatively different regimes of photon antibunching are present for *weak* and *strong* single photon-trion coupling. We find that single photon emission from trion polaritons becomes experimentally feasible in state-of-the-art transition metal dichalcogenide setups. This can foster the development of quantum polaritonics using 2D monolayers as a material platform.

DOI: 10.1103/PhysRevLett.125.197402

Introduction.—Exciton polaritons are hybrid quasiparticles formed in optical microcavities in the regime of strong light-matter coupling. Their unique properties related to the composite nature lead to a dramatic enhancement of the nonlinear optical response and enable the observation of quantum collective phenomena at relatively high temperatures [1,2]. Examples include the observation of a polariton Bose-Einstein condensate and polariton lasing [3–5], topological defects such as solitons [6–11], and quantized vortices [12–16], and many others [17–19].

For conventional GaAs [4] and CdTe [3] systems polaritonic nonlinearities mainly stem from exciton-exciton scattering processes, governed by the Coulomb exchange of electrons and holes [20,21]. However, another important contribution comes from phase-space filling effects related to the composite nature of excitons [22,23], also known as nonlinear saturation effects [21]. In GaAs these effects were shown to be negligible at moderate pump powers [21], but can become significant in certain cases [24]. They also govern the transition from strong to weak coupling at large pump powers [25,26] and dominate the nonlinear response of Frenkel excitons [27–29].

One of the most promising platforms for polaritonics is represented by transition metal dichalcogenide (TMD) monolayers [30–34]. TMD excitons have extremely large binding energies and oscillator strengths as compared to excitons in conventional semiconductors, dominating an optical response even at room temperature [35–37]. Moreover, it is also important that optical spectra of TMD monolayers reveal robust trion [36–41] and biexciton [42,43] peaks, as well as excited exciton states [44–47]. Trion-based response usually dominates at small exciton densities, and at high densities ($> 10^{12}$ cm^{-2}) the exciton-polaron effects become important [48–50]. In the polariton regime, the exciton-based nonlinear energy shift [51,52] together with dissipative nonlinearity coming from exciton-exciton annihilation [53] were reported, and enhancement of nonlinearity in the cooperative coupling regime [54] was proposed. Recent experimental study revealed the appearance of trion polaritons in a $MoSe_2$ monolayer and large saturative nonlinearity [55].

Recently, the quality improvement of optical microcavities has much prolonged the lifetime of exciton polaritons [56], thus allowing to observe the first signatures of entering the quantum regime [57]. The current state-of-the art is represented by weak antibunching of 0.95 [57,58]. However, the possibility to obtain stronger antibunching is ultimately limited by insufficient Kerr-type nonlinearity coming from the effective exciton-exciton interaction [59]. This hinders the associated development of quantum polaritonics, and qualitatively new ideas are needed in order to propose how one can increase dramatically the nonlinear response of the system on single quantum level. Potential solutions correspond to using the effects of quantum interference in double pillar systems without increasing the interaction constant itself [60–65], or enhancing the interaction in dipolariton systems [66–68].

In this Letter we study trion polaritons in TMD monolayers and show that their composite nature results in a highly nonlinear optical response. We build the full non-perturbative quantum theory of the phase-space filling effects. In particular, we find regions of parameters where

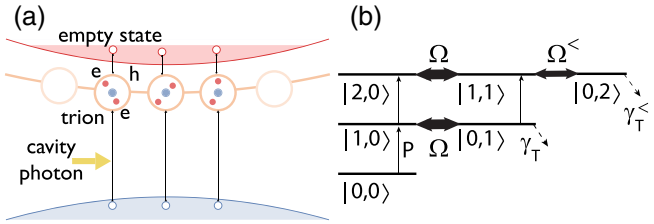

FIG. 1. (a) Sketch of trion excitations. A cavity photon creates an electron-hole pair and captures an electron from the conduction band to form a trion complex. (b) Energy level scheme in photon-trion basis $|N_C, N_T\rangle$, where the direct excitation path $|0,0\rangle \rightarrow |1,0\rangle \rightarrow |2,0\rangle$ destructively interferes with the trion-mediated path. The effective nonlinearity comes from the reduced coupling $\Omega^<$ in the presence of two trions.

unconventional *saturation-based blockade* can be achieved, as well as describe conventional blockade attainable at large single photon-trion couplings. We show that in state-of-the-art TMD polariton structures the antibunching of $g^{(2)}(0) < 0.1$ can be achieved. Plotting the optical spectrum of the system at increasing pump power, we also find the conditions for the transition between strong and weak light-matter coupling regimes.

The model.—We aim to build a quantum theory of trion polaritons and study their optical properties. We start by considering a planar semiconductor which is initially electron doped, and consider a dilute electron gas limit where trions dominate. We note that the theory is not directly applicable to a regime of large densities, where crossover to the exciton-polaron regime happens [49,50]. In the latter discussion we stress the applicability range, and note that a low density regime is beneficial for achieving antibunching. Optically excited electron-hole (e-h) pairs can interact with available free electrons and form a bound trion state [Fig. 1(a)]. The corresponding creation operator for this composite particle reads [69]

$$\hat{T}^\dagger_{\mathbf{K},\mathbf{s}} = \sum_{\mathbf{k}_1,\mathbf{k}_2,\mathbf{s}} \phi_{\mathbf{K},\mathbf{k}_1,\mathbf{k}_2;\mathbf{s}} \hat{a}^\dagger_{\mathbf{k}_1,s_1} \hat{a}^\dagger_{\mathbf{k}_2,s_2} \hat{b}^\dagger_{\mathbf{K}-\mathbf{k}_1-\mathbf{k}_2,s_3}, \quad (1)$$

where the trion wave function $\phi_{\mathbf{K},\mathbf{k}_1,\mathbf{k}_2;\mathbf{s}}$ is separated into a center-of-mass part with momentum $\mathbf{K}$, and the relative motion part described by the relative motion wave function $\phi_{\mathbf{k}_1,\mathbf{k}_2}$. Here, $\hat{a}^\dagger_{\mathbf{k},s_j}$ and $\hat{b}_{\mathbf{k},s_j}$ are fermionic creation operators for electrons and holes, the indices s_j correspond to the spins of individual fermions which define the spin configuration of a trion complex (denoted by the index $\mathbf{s}$), which can be a singlet or a triplet. In the following we consider only dominant trions in a singlet configuration, omitting spin indices for brevity.

The full excitation process relies on taking an electron from the Fermi sea by a photocreated e-h pair, where an empty electron state is left in the conduction band [Fig. 1(a)]. This process can be conveniently described by the generation of the quasibosonic excitation in the system from the vacuum state $|\varnothing\rangle$ corresponding to the Fermi sea, and we consider the low temperature case of a degenerate electron gas. The process is described by the excitation wave function $\hat{B}^\dagger_{\mathbf{K}}|\varnothing\rangle = (1/\sqrt{N_s})\sum_{\mathbf{k}} \hat{T}^\dagger_{\mathbf{K}+\mathbf{k}}\hat{a}_{\mathbf{k}}|\varnothing\rangle$ [70,71] where N_s is a number of free electrons available for a trion creation. As the excitation operator $\hat{B}^\dagger_{\mathbf{K}}$ contains four fermionic operators, it represents a composite boson with commutation relation $[\hat{B}_{\mathbf{q}'}, \hat{B}^\dagger_{\mathbf{q}}] = \delta_{\mathbf{q}',\mathbf{q}} - \hat{D}_{\mathbf{q}',\mathbf{q}}$, where operator $\hat{D}_{\mathbf{q}',\mathbf{q}}$ represents the deviation from bosonicity. For tightly bound trions present in TMD monolayers the trion operators [Eq. (1)] can be treated as fermions, as their fine structure is only revealed at densities comparable to the inverse area of a trion $(\pi a_T^2)^{-1}$. In this case, the deviation operator corresponds to the fraction of trions formed out of the Fermi sea, $\hat{D}_{\mathbf{q}',\mathbf{q}} = \sum_{\mathbf{k}} \hat{T}^\dagger_{\mathbf{q}+\mathbf{k}}\hat{T}_{\mathbf{q}'+\mathbf{k}}/N_s$. This makes trion-polariton excitations prone to the phase space filling effects and can lead to the saturation of light-matter coupling. At the same time, we remind the reader that $\hat{B}_{\mathbf{K}}$ is not a bound state, and thus exhibits different statistics as compared to exciton polaritons [22,24], resembling more the case of intersubband polaritons [72–74] and Frenkel excitons [75].

The Hamiltonian of the system can be written as the sum of three terms, $\hat{\mathcal{H}} = \hat{\mathcal{H}}_0 + \hat{\mathcal{H}}_{\text{coupl}} + \hat{\mathcal{H}}_{\text{T-T}}$. Here, $\hat{\mathcal{H}}_0$ describes noninteracting cavity photons, electrons, and trions. $\hat{\mathcal{H}}_{\text{coupl}}$ describes the processes of light-matter coupling, and $\hat{\mathcal{H}}_{\text{T-T}}$ describes Coulomb trion-trion scattering. In this Letter we focus on the mechanism of nonlinearity stemming from the saturation effects related to the Pauli exclusion principle, and neglect the latter term responsible for higher-order Coulomb effects. We also note that higher-order effects can appear due to hybridization with biexcitons [42,76,77], while for the weak pump and significant separation in energy they will play a minor role. The light-matter coupling Hamiltonian can be expressed in terms of the photonic operators $\hat{c}_{\mathbf{q}}$ and operators of quasibosonic excitations $\hat{B}^\dagger_{\mathbf{k}}$, reading $\hat{\mathcal{H}}_{\text{coupl}} = (\Omega/2)\sum_{\mathbf{k}}(\hat{B}^\dagger_{\mathbf{k}}\hat{c}_{\mathbf{k}} + \hat{B}_{\mathbf{k}}\hat{c}^\dagger_{\mathbf{k}})$, where $\Omega = g_0\sqrt{N_s}\sum_{\mathbf{k}_1,\mathbf{k}_2}\phi_{\mathbf{k}_1,\mathbf{k}_2}$ is a Rabi energy for coupling between the collective trion mode and cavity photons (accounting for the trion localization), with g_0 being a valence-to-conduction band transition matrix element.

The total number of excitations (photons plus trions) in the system is conserved. Thus, we can split the associated Hilbert-Fock space of the problem into separate manifolds corresponding to the different numbers of the excitations N, and then diagonalize each block separately. For this, let us define the matrix element $\mathcal{M}^{m,n}_{m',n'} := \langle m', n'|\hat{\mathcal{H}}|m, n\rangle$, where $|N_C, N_T\rangle$ represents a state with N_C photons (bosons) and N_T quasibosonic trion excitations. The Hamiltonian describing $N = N_C + N_T - 1$ particles is represented by the matrix

$$\hat{H}_N = \begin{bmatrix} \mathcal{M}^{N_C,N_T-1}_{N_C,N_T-1} & \mathcal{M}^{N_C-1,N_T}_{N_C,N_T-1} \\ \mathcal{M}^{N_C,N_T-1}_{N_C-1,N_T} & \mathcal{M}^{N_C-1,N_T}_{N_C-1,N_T} \end{bmatrix}. \quad (2)$$

The matrix elements entering the expression above can be calculated elementwise, properly accounting for the composite nature of the particles. The diagonal elements read $\mathcal{M}^{N_C,N_T-1}_{N_C,N_T-1} = N_C\omega_{\rm cav} + \omega_T(N_T-1)$, where $\omega_{\rm cav}$ is the energy of the photonic cavity mode, and ω_T corresponds to the energy difference between electron and trion energies. The crucial point of derivation corresponds to the off-diagonal elements, coming from the strong light-matter coupling Hamiltonian $\hat{\mathcal{H}}_{\rm coupl}$, which read [78]

$$\mathcal{M}^{N_C-1,N_T}_{N_C,N_T-1} = \frac{\Omega}{2}\sqrt{N_C N_T\left(1-\frac{N_T}{N_s+1}\right)}\sqrt{\frac{N_s}{N_s+1}} \times\left[1-(-1)^{N_T}\frac{(N_s-N_T)!N_T!}{N_s!}\right]. \quad (3)$$

Importantly, expression Eq. (3) (i) holds for arbitrary $N_T \le N_s$; (ii) is valid for highly nonlinear case of $N_s = 1$ (corresponding to a qubit) [79]; (iii) provides physical result for singly occupied mode $N_T = 1$, unlike for Holstein-Primakoff approach [80–82] widely used for large N_T but failing in this limit crucial for quantum statistics.

Trion-polariton spectrum.—Once blocks $\hat{H}_N$ are known, the polariton energies can be found separately for each N. We assume the monomode approximation corresponding to an effectively 0D open microcavity [31], such that only zero momenta photons are considered, $\hat{c} \coloneqq \hat{c}_{\mathbf{k}\to 0}$, $\hat{B} \coloneqq \hat{B}_{\mathbf{k}\to 0}$, $\hat{H}_{\rm coupl} \coloneqq (\Omega/2)(\hat{B}^\dagger\hat{c} + \hat{B}\hat{c}^\dagger)$. We consider the system driven by a strong coherent pulse, such that initial particle distribution corresponds to a coherent state for the photonic field given by the Poisson distribution with amplitude α, while the trion mode remains unoccupied. We calculate the corresponding transmission spectrum $S(\omega)$ (see Ref. [78], Sec. B, and Refs. [83–85]) for an increasing total number of photons $N_C = |\alpha|^2$. The cavity output, modified by the strong coupling to trions, is then monitored in the transmission geometry. The results are shown in Fig. 2(a), where we considered zero cavity-trion detuning $\delta = \omega_{\rm cav} - \omega_T$, fixed dissipation rates of $\gamma_c = \gamma_T = 0.05\Omega$, and $N_s = 100$ available electronic states. For small N_C the two trion-polariton peaks are clearly visible, representing the expected Rabi doublet. As N_C increases the number of transitions grows and the distance between the peaks decreases [see Eq. (3)]. Finally, at large occupations $N_C > 100$ the two peaks merge and the broad band of transitions is visible in the spectrum. This behavior was recently observed experimentally in the $MoSe_2$ setup [55]. To track the collapse of the strong coupling, we plot peak positions as a function of pump (N_C) for different dissipation rates [Fig. 2(b)]. At large decay rates ($\gamma/\Omega = 0.1$) the collapse is shifted to smaller N_C values, while for narrow lines it saturates at $N_C = N_s$.

Antibunching.—To calculate the quantum statistics for the cavity photons we consider the finite Hilbert space with

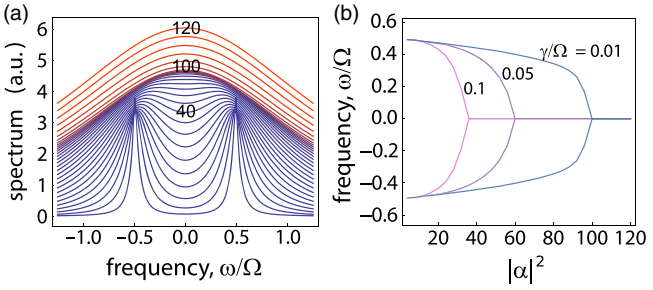

FIG. 2. (a) Absorption spectrum of a trion-polariton system for various photon numbers $N_C = |\alpha|^2$ being injected to the system by short coherent optical pulse. The parameters are fixed to $N_s = 100$ available electronic states, $\gamma_{c,T} = 0.05\Omega$, and we work at zero photon-trion detuning (values of $N_C = \{40, 100, 120\}$ are highlighted). (b) Spectral peak locations for lower and upper polariton modes are shown as a function of drive, and reveal the collapse of strong coupling.

matrix elements modified due to the phase space filling as shown in Eq. (3). We consider the case of a weak coherent cw pump with frequency ω_p and strength P detuned from the cavity mode by $\Delta = \omega_{\rm cav} - \omega_p$. The dynamics for the system is studied using the master equation approach, where Lindblad dissipation terms with collapse operators $\sqrt{\gamma_c}\hat{c}$ and $\sqrt{\gamma_T}\hat{B}$ are introduced [78]. As we focus on the regime of few quanta, N_C and N_T are truncated in the way that higher states are negligibly populated (we consider the range of pumps for which $N_C, N_T < 10$).

To characterize the statistics of the cavity output we calculate the second-order coherence function at finite time delay τ, $g^{(2)}(\tau) = \langle\hat{c}^\dagger(0)\hat{c}^\dagger(\tau)\hat{c}(\tau)\hat{c}(0)\rangle/\langle\hat{c}^\dagger\hat{c}\rangle^2$, as well as steady state intracavity occupation $n_{\rm cav} = \langle\hat{c}^\dagger\hat{c}\rangle$. The results are shown in Fig. 3, where for brevity we concentrate on the case of equal decay rates $\gamma_c = \gamma_T = \gamma$ and zero trion-photon detuning $\omega_{\rm cav} = \omega_T$ (see Ref. [78] for full characterization). Studying the dependence of second-order coherence at zero delay $g^{(2)}(0)$ on the pump detuning Δ we reveal two qualitatively different regimes of antibunching coming from the optical saturation of the trion-photon coupling. At small single trion coupling, $g_c = \Omega/\sqrt{N_s}$ being comparable with cavity and trion linewidth, we find the region of pronounced antibunching which can be attributed to the unconventional photon blockade [60,61], where due to destructive interference the two-photon occupation vanishes [Fig. 3(a)]. Namely, there are two excitation paths to populate the two-photon state—one from direct coherent excitation, and the second via the alternative root through the trion mode [Fig. 1(b)]. For certain optimal conditions the two interfere destructively (see Ref. [78], Sec. D, for optimal parameters), leading to a largely reduced two-photon probability. The process requires the pump to be nearly resonant with the cavity mode and $g_c/\gamma \sim 1$, and notably the optimal pump position does not depend on g_c. Already at $g_c/\gamma = 2$ the $\Delta \approx 0$

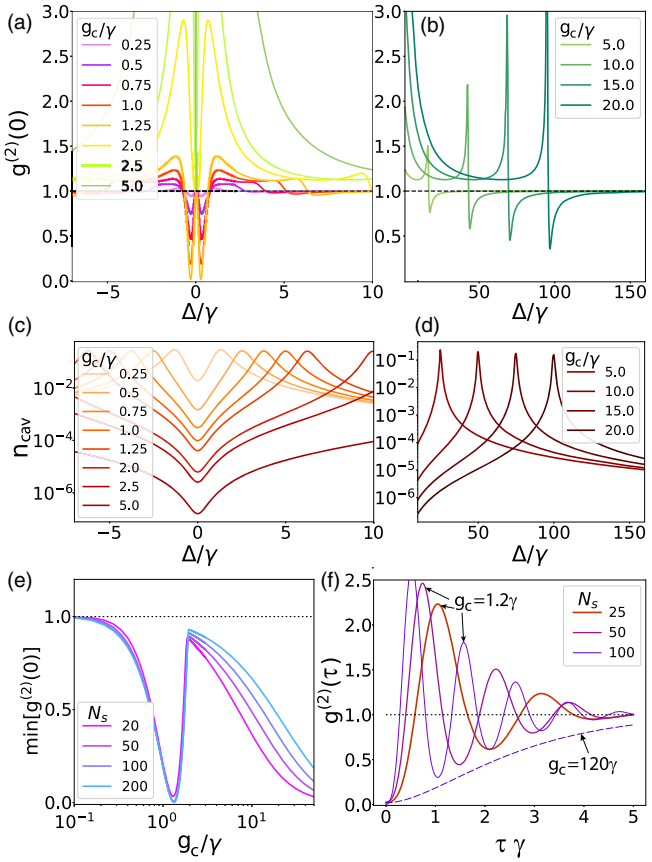

FIG. 3. Second order coherence at zero delay for trion-polariton system vs different parameters. (a),(b) $g^{(2)}(0)$ for cavity photons plotted as a function of pump detuning $\Delta = \omega_{\rm cav} - \omega_p$ for different values of a single trion-photon coupling $g_c = \Omega/\sqrt{N_s}$. In (a) the unconventional blockade window at $\Delta \approx 0$ and small $g_c \approx \gamma$ is shown, and (b) shows the conventional regime at $\Delta \approx \omega_L$ and large $g_c/\gamma \gg 1$. (c),(d) Cavity occupations corresponding to the same parameters as in (a) and (b). (e) Minimal $g^{(2)}(0)$ considered over wide detuning Δ range, plotted as a function of g_c, showing both unconventional and conventional blockade regions for various electron numbers N_s. (f) Time-delayed second order coherence $g^{(2)}(\tau)$ where solid curves depict results for $g_c = 1.2\gamma$ at optimal detuning and increasing N_s. Dashed curve corresponds to the case of conventional blockade ($g_c = 120\gamma$ and $N_s = 100$).

antibunching window disappears, and instead the single photon emission at lower polariton frequency $\omega_p \approx \omega_L = (\omega_{\rm cav} + \omega_T)/2 - \sqrt{\Omega^2 + \delta^2}/2$ emerges. In Fig. 3(b) this corresponds to the minimum at $\Delta/\gamma \approx \Omega/2$ which shifts with g_c. The Fano-lineshape profile of $g^{(2)}(0)$ [Fig. 3(b)] and requirement of the strong single trion-photon coupling $g_c/\gamma \gg 1$ allows us to attribute it to conventional blockade, comparable to antibunching in Kerr-type nonlinear systems [59]. The probability of the single photon emission, being proportional to cavity occupation $n_{\rm cav}$, is plotted in Figs. 3(c) and 3(d). As the unconventional antibunching window lies in the middle of the polaritonic spectra, the associated occupations lie in the 10^{-3}–10^{-4} range [Fig. 3(c)], for relevant $g_c/\gamma \sim 0.5$–1.2 values ($P/\gamma = 0.5$ is considered). For the ω_L-resonant pump the occupation peaks at 0.1 values for minimal $g^{(2)}(0)$ [Fig. 3(d)], at the expense of weaker antibunching and the large g_c/γ requirement. The performance in both regimes can be further characterized by plotting minimized $g^{(2)}(0)$ for both detuning windows as a function of light-matter coupling g_c and number of electrons N_s [Fig. 3(e)]. While in the unconventional regime low $g^{(2)}(0)$ holds well for $g_c/\gamma < 2$ and does not depend on N_s, the conventional case for $g_c/\gamma > 2$ shows N_s dependence where low electron concentration is favored. Finally, the important dependence of the single photon emission is a finite delay response, which defines how well the emitted single photon can be resolved [86]. As expected for the interference effect, the unconventional trion-polariton blockade plotted for optimal Δ and $g_c/\gamma = 1.2$ shows oscillations in $g^{(2)}(\tau)$ with the period inversely proportional to $\sqrt{N_s}$, where the antibunching region shrinks as N_s grows [Fig. 3(f)], while remaining a significant portion of γ^{-1} even for large occupation $N_s = 100$. We compare it to the conventional blockade at two-orders larger coupling $g_c = 120\gamma$ ($N_s = 100$), which does not show oscillations, yet increases with τ.

Discussion.—To get the quantitative estimates for trion-based antibunching in TMD materials, the characteristic strength of light-matter coupling between a cavity photon and a trion can be estimated as $g_c = g_0\chi_T$, where g_0 is the bare e-h coupling constant, and χ_T is a trion confinement coefficient coming from integrating the relative motion wave function. We adopt the approach from Refs. [87–90] and consider the standard Chandrasekhar-type wave function for the trion with two variational parameters [69], which was shown to work well for nearly equal electron-hole effective masses [38]. In this case, the confinement coefficient becomes

$$\chi_T = [8(\lambda_1^2+\lambda_2^2)^2(\lambda_1+\lambda_2)^4/\{\lambda_1^2\lambda_2^2(\lambda_1+\lambda_2)^4 + 16\lambda_1^4\lambda_2^4\}]^{1/2}, \tag{4}$$

with λ_1 and λ_2 being variational parameters corresponding to the effective radii of electrons in a trion (which can be understood as excitonlike shell and outer electron shell properties). Considering $\lambda_2 > \lambda_1$, the limit of $\lambda_2/\lambda_1 \gg 1$ is favored for achieving large χ_T. The bare electron-hole pair coupling can be calculated as [91]

$$g_0 = e p_{cv}\sqrt{\frac{\eta^2\hbar^2}{2\epsilon\epsilon_0 m_0^2\omega_0 L_{\rm cav} A}} = \sqrt{\frac{\eta^2\hbar^2 e^2}{\epsilon\epsilon_0\mu L_{\rm cav} A}}, \tag{5}$$

where e is an electron charge, p_{cv} is an interband transition matrix element, η accounts for TMD placement in the cavity ($\eta = 1$ corresponds to an antinode), ϵ is dielectric medium permittivity, ϵ_0 is vacuum permittivity, m_0 is a free

electron mass, ω_0 is a transition energy, L_{cav} is a cavity length, $\mu = m_0(1/m_e + 1/m_h)^{-1}$ is the reduced electron-hole pair mass, and A is the sample area.

As a particular example we consider a $MoSe_2$ monolayer inside an open cavity. The parameters of a standard setup are chosen as effective cavity length $L_{\mathrm{cav}} = 1$ μm, cavity area of $A = 1$ μm^2, electron density of $n_s = N_s/A = 10^{10}$ cm^{-2}, and optical linewidth of $\gamma_c = 50$ μeV. The effective masses of the electron and hole in $MoSe_2$ $m_e = 0.8$ and $m_h = 0.84$ [92], and Eq. (5) gives $g_0 = 0.058$ meV ($\eta = 1$), as expected for a direct band gap semiconductor [93]. Performing the variational procedure for the relevant case of $MoSe_2$ on hexagonal boron nitride (h-BN) the trion radii are $\lambda_1 = 0.87$ nm and $\lambda_2 = 2.54$ nm, providing the enhancement coefficient of $\chi_T = 7.35$. As we consider dilute electron gas, the Fermi energy $E_F = 0.03$ meV is much smaller than the trion binding energy of $E_b^T = 20$ meV. The condition $E_F/E_b^T \ll 1$ confirms that we are in the trion-dominated regime [49]. The nonradiative decay rate for trions was measured in h-BN encapsulated samples $\gamma_T = 0.26$ meV due to inhomogeneous exciton broadening [94]. Considering the TMD monolayer placed outside of the antinode with $\eta = 0.6$, yielding $g_c = 0.256$ meV, the setup can provide unconventional antibunching of $g^{(2)}_{\mathrm{MoSe_2}}(0) = 0.064$ with $n_{\mathrm{cav}} = 0.00013$. Improving the system, trion nonradiative decay can be reduced to $\gamma_T \sim 10$ μeV at 1 K temperature given by phonon interactions only [94], and we note that the cavity linewidth $\gamma_c \sim 10$ μeV was already realized in state-of-the-art setups [95,96]. Thus, for the optimally coupled layer ($\eta = 1$) the conventional antibunching value of $g^{(2)}_{\mathrm{MoSe_2}}(0) = 0.091$ can be obtained. One can compare this to the potential state-of-the-art GaAs sample with a 2.3 μm diameter micropillar cavity of the same effective area, where the exciton-exciton interaction-based Kerr blockade [59] can give $g^{(2)}_{\mathrm{GaAs}}(0) = 0.92$ for the same values of broadening, the limit nearly approached experimentally, where antibunching at 0.95 level was reported [57,58].

Conclusions.—We developed a theory of quantum nonlinear optical response of trion polaritons fully accounting for their composite nature and related phase-space filling effects up to infinite order. We observed and described quantitatively the collapse of the strong light-matter coupling with increase of the optical pump. We studied the effect of quantum correlations in the system, and revealed the rich phenomenology where both unconventional and conventional blockade can be studied in regimes of weak and strong single trion-photon coupling, correspondingly. We found that strong antibunching of the photonic emission is possible with TMD monolayers put in an open microcavity, being accessible in modern and near-term setups.

We would like to thank Alexey Kavokin and Ataç Imamoglu for the useful discussions. The work was supported by the Government of the Russian Federation through the Megagrant 14.Y26.31.0015, ITMO Fellowship and Professorship Program, and the part of the work related to the numerical analysis of the predicted effects was supported by the Russian Science Foundation Project No. 18-72-10110. O. K. thanks UK EPSRC New Investigator Award under the Agreement No. EP/V00171X/1 for the support.

[1] I. Carusotto and C. Ciuti, Rev. Mod. Phys. **85**, 299 (2013).
[2] T. Byrnes, N. Y. Kim, and Y. Yamamoto, Nat. Phys. **10**, 803 (2014).
[3] J. Kasprzak, M. Richard, S. Kundermann, A. Baas, P. Jeambrun, J. M. J. Keeling, F. M. Marchetti, M. H. Szymanska, R. Andre, J. L. Staehli, V. Savona, P. B. Littlewood, B. Deveaud, and L. Si Dang, Nature (London) **443**, 409 (2006).
[4] R. Balili, V. Hartwell, D. Snoke, and K. West, Science **316**, 1007 (2007).
[5] C. Schneider, A. Rahimi-Iman, N. Y. Kim, J. Fischer, I. G. Savenko, M. Amthor, M. Lermer, A. Wolf, L. Worschech, V. D. Kulakovskii, I. A. Shelykh, M. Kamp, S. Reitzenstein, A. Forchel, Y. Yamamoto, and S. Höfling, Nature (London) **497**, 348 (2013).
[6] A. Amo, S. Pigeon, D. Sanvitto, V. G. Sala, R. Hivet, I. Carusotto, F. Pisanello, G. Leménager, R. Houdré, E. Giacobino, C. Ciuti, and A. Bramati, Science **332**, 1167 (2011).
[7] M. Sich, D. N. Krizhanovskii, M. S. Skolnick, A. V. Gorbach, R. Hartley, D. V. Skryabin, E. A. Cerda-Méndez, K. Biermann, R. Hey, and P. V. Santos, Nat. Photonics **6**, 50 (2012).
[8] R. Hivet, H. Flayac, D. D. Solnyshkov, D. Tanese, T. Boulier, D. Andreoli, E. Giacobino, J. Bloch, A. Bramati, G. Malpuech, and A. Amo, Nat. Phys. **8**, 724 (2012).
[9] J. K. Chana, M. Sich, F. Fras, A. V. Gorbach, D. V. Skryabin, E. Cancellieri, E. A. Cerda-Méndez, K. Biermann, R. Hey, P. V. Santos, M. S. Skolnick, and D. N. Krizhanovskii, Phys. Rev. Lett. **115**, 256401 (2015).
[10] T. Boulier, H. Teras, D. D. Solnyshkov, Q. Glorieux, E. Giacobino, G. Malpuech, and A. Bramati, Sci. Rep. **5**, 9230 (2015).
[11] D. R. Gulevich, D. Yudin, D. V. Skryabin, I. V. Iorsh, and I. A. Shelykh, Sci. Rep. **7**, 1780 (2017).
[12] Yu. G. Rubo, Phys. Rev. Lett. **99**, 106401 (2007).
[13] K. G. Lagoudakis, M. Wouters, M. Richard, A. Baas, I. Carusotto, R. Andre, L. S. Dang, and B. Deveaud-Pledran, Nat. Phys. **4**, 706 (2008).
[14] G. Tosi, G. Christmann, N. G. Berloff, P. Tsotsis, T. Gao, Z. Hatzopoulos, P. G. Savvidis, and J. J. Baumberg, Nat. Commun. **3**, 1243 (2012).
[15] T. Gao, O. A. Egorov, E. Estrecho, K. Winkler, M. Kamp, C. Schneider, S. Höfling, A. G. Truscott, and E. A. Ostrovskaya, Phys. Rev. Lett. **121**, 225302 (2018).
[16] M.-S. Kwon, B. Y. Oh, S.-H. Gong, J.-H. Kim, H. K. Kang, S. Kang, J. D. Song, H. Choi, and Y.-H. Cho, Phys. Rev. Lett. **122**, 045302 (2019).

[17] For a review on polaritonic devices see: T. C. H. Liew, I. A. Shelykh, and G. Malpuech, Physica (Amsterdam) **43E**, 1543 (2011).
[18] T. Espinosa-Ortega and T. C. H. Liew, Phys. Rev. B **87**, 195305 (2013).
[19] A. Opala, S. Ghosh, T. C. H. Liew, and M. Matuszewski, Phys. Rev. Applied **11**, 064029 (2019).
[20] C. Ciuti, V. Savona, C. Piermarocchi, A. Quattropani, and P. Schwendimann, Phys. Rev. B **58**, 7926 (1998).
[21] F. Tassone and Y. Yamamoto, Phys. Rev. B **59**, 10830 (1999).
[22] M. Combescot, O. Betbeder-Matibet, and F. Dubin, Phys. Rep. **463**, 215 (2008).
[23] S.-Y. Shiau and M. Combescot, Phys. Rev. Lett. **123**, 097401 (2019).
[24] A. S. Brichkin, S. I. Novikov, A. V. Larionov, V. D. Kulakovskii, M. M. Glazov, C. Schneider, S. Hofling, M. Kamp, and A. Forchel, Phys. Rev. B **84**, 195301 (2011).
[25] R. Butte, G. Delalleau, A. I. Tartakovskii, M. S. Skolnick, V. N. Astratov, J. J. Baumberg, G. Malpuech, A. Di Carlo, A. V. Kavokin, and J. S. Roberts, Phys. Rev. B **65**, 205310 (2002).
[26] D. Bajoni, E. Semenova, A. Lemaitre, S. Bouchoule, E. Wertz, P. Senellart, S. Barbay, R. Kuszelewicz, and J. Bloch, Phys. Rev. Lett. **101**, 266402 (2008).
[27] K. S. Daskalakis, S. A. Maier, R. Murray, and S. Kéna-Cohen, Nat. Mater. **13**, 271 (2014).
[28] T. Yagafarov, D. Sannikov, A. Zasedatelev, K. Georgiou, A. Baranikov, O. Kyriienko, I. Shelykh, L. Gai, Z. Shen, D. Lidzey, and P. Lagoudakis, Communications in Physics **3**, 18 (2020).
[29] S. Betzold, M. Dusel, O. Kyriienko, C. P. Dietrich, S. Klembt, J. Ohmer, U. Fischer, I. A. Shelykh, C. Schneider, and S. Höfling, ACS Photonics **7**, 384 (2020).
[30] X. Liu, T. Galfsky, Z. Sun, F. Xia, E.-C. Lin, Y.-H. Lee, S. Kéna-Cohen, and V. M. Menon, Nat. Photonics **9**, 30 (2015).
[31] S. Dufferwiel, T. P. Lyons, D. D. Solnyshkov, A. A. P. Trichet, F. Withers, S. Schwarz, G. Malpuech, J. M. Smith, K. S. Novoselov, M. S. Skolnick, D. N. Krizhanovskii, and A. I. Tartakovskii, Nat. Photonics **11**, 497 (2017).
[32] N. Lundt, A. Marynski, E. Cherotchenko, A. Pant, X. Fan, S. Tongay, G. Sek, A. V. Kavokin, S. Höfling, and C. Schneider, 2D Mater. **4**, 015006 (2017).
[33] C. Schneider, M. M. Glazov, T. Korn, S. Hofling, and B. Urbaszek, Nat. Commun. **9**, 2695 (2018).
[34] L. Zhang, R. Gogna, W. Burg, E. Tutuc, and H. Deng, Nat. Commun. **9**, 713 (2018).
[35] G. Wang, A. Chernikov, M. M. Glazov, T. F. Heinz, X. Marie, T. Amand, and B. Urbaszek, Rev. Mod. Phys. **90**, 021001 (2018).
[36] K. F. Mak, K. He, C. Lee, G. H. Lee, J. Hone, T. F. Heinz, and J. Shan, Nat. Mater. **12**, 207 (2013).
[37] J. S. Ross, S. Wu, H. Yu, N. J. Ghimire, A. M. Jones, G. Aivazian, J. Yan, D. G. Mandrus, D. Xiao, W. Yao, and X. Xu, Nat. Commun. **4**, 1474 (2013).
[38] E. Courtade, M. Semina, M. Manca, M. M. Glazov, C. Robert, F. Cadiz, G. Wang, T. Taniguchi, K. Watanabe, M. Pierre, W. Escoffier, E. L. Ivchenko, P. Renucci, X. Marie, T. Amand, and B. Urbaszek, Phys. Rev. B **96**, 085302 (2017).
[39] N. Lundt, E. Cherotchenko, O. Iff, X. Fan, Y. Shen, P. Bigenwald, A. V. Kavokin, S. Höfling, and C. Schneider, Appl. Phys. Lett. **112**, 031107 (2018).
[40] K. F. Mak, K. He, C. Lee, G. H. Lee, J. Hone, T. F. Heinz, and J. Shan, Nat. Mater. **12**, 207 (2013).
[41] J. S. Ross, S. Wu, H. Yu, N. J. Ghimire, A. M. Jones, G. Aivazian, J. Yan, D. G. Mandrus, D. Xiao, W. Yao, and X. Xu, Nat. Commun. **4**, 1474 (2013).
[42] Y. You, X.-X. Zhang, T. C. Berkelbach, M. S. Hybertsen, D. R. Reichman, and T. F. Heinz, Nat. Phys. **11**, 477 (2015).
[43] P. Nagler, M. V. Ballottin, A. A. Mitioglu, M. V. Durnev, T. Taniguchi, K. Watanabe, A. Chernikov, C. Schuller, M. M. Glazov, P. C. M. Christianen, and T. Korn, Phys. Rev. Lett. **121**, 057402 (2018).
[44] A. Chernikov, T. C. Berkelbach, H. M. Hill, A. Rigosi, Y. Li, O. B. Aslan, D. R. Reichman, M. S. Hybertsen, and T. F. Heinz, Phys. Rev. Lett. **113**, 076802 (2014).
[45] J. Zipfel, J. Holler, A. A. Mitioglu, M. V. Ballottin, P. Nagler, A. V. Stier, T. Taniguchi, K. Watanabe, S. A. Crooker, P. C. M. Christianen, T. Korn, and A. Chernikov, Phys. Rev. B **98**, 075438 (2018).
[46] B. Han, C. Robert, E. Courtade, M. Manca, S. Shree, T. Amand, P. Renucci, T. Taniguchi, K. Watanabe, X. Marie, L. E. Golub, M. M. Glazov, and B. Urbaszek, Phys. Rev. X **8**, 031073 (2018).
[47] C.-K. Yong, M. I. B. Utama, C. S. Ong, T. Cao, E. C Regan, J. Horng, Y. Shen, H. Cai, K. Watanabe, T. Taniguchi, S. Tongay, H. Deng, A. Zettl, S. G Louie, and F. Wang, Nat. Mater. **18**, 1065 (2019).
[48] M. Sidler, P. Back, O. Cotlet, A. Srivastava, T. Fink, M. Kroner, E. Demler, and A. Imamoglu, Nat. Phys. **13**, 255 (2017).
[49] D. K. Efimkin and A. H. MacDonald, Phys. Rev. B **95**, 035417 (2017).
[50] Y.-C. Chang, S.-Y. Shiau, and M. Combescot, Phys. Rev. B **98**, 235203 (2018).
[51] V. Shahnazaryan, I. Iorsh, I. A. Shelykh, and O. Kyriienko, Phys. Rev. B **96**, 115409 (2017).
[52] F. Barachati, A. Fieramosca, S. Hafezian, Jie Gu, B. Chakraborty, D. Ballarini, L. Martinu, V. Menon, D. Sanvitto, and S. Kéna-Cohen, Nat. Nanotechnol. **13**, 906 (2018).
[53] N. Kumar, Q. Cui, F. Ceballos, D. He, Y. Wang, and H. Zhao, Phys. Rev. B **89**, 125427 (2014).
[54] D. S. Wild, E. Shahmoon, S. F. Yelin, and M. D. Lukin, Phys. Rev. Lett. **121**, 123606 (2018).
[55] R. P. A. Emmanuele, M. Sich, O. Kyriienko, V. Shahnazaryan, F. Withers, A. Catanzaro, P. M. Walker, F. A. Benimetskiy, M. S. Skolnick, A. I. Tartakovskii, I. A. Shelykh, and D. N. Krizhanovskii, Nat. Commun. **11**, 3589 (2020).
[56] B. Nelsen, G. Liu, M. Steger, D. W. Snoke, R. Balili, K. West, and L. Pfeiffer, Phys. Rev. X **3**, 041015 (2013).
[57] G. Munoz-Matutano, A. Wood, M. Johnsson, X. Vidal, B. Q. Baragiola, A. Reinhard, A. Lemaitre, J. Bloch, A. Amo, G. Nogues, B. Besga, M. Richard, and T. Volz, Nat. Mater. **18**, 213 (2019).

[58] A. Delteil, T. Fink, A. Schade, S. Höfling, C. Schneider, and A. Imamoglu, Nat. Mater. **18**, 219 (2019).
[59] A. Verger, C. Ciuti, and I. Carusotto, Phys. Rev. B **73**, 193306 (2006).
[60] T. C. H. Liew and V. Savona, Phys. Rev. Lett. **104**, 183601 (2010).
[61] M. Bamba, A. Imamoglu, I. Carusotto, and C. Ciuti, Phys. Rev. A **83**, 021802(R) (2011).
[62] H. J. Snijders, J. A. Frey, J. Norman, H. Flayac, V. Savona, A. C. Gossard, J. E. Bowers, M. P. van Exter, D. Bouwmeester, and W. Loffler, Phys. Rev. Lett. **121**, 043601 (2018).
[63] H. Flayac and V. Savona, Phys. Rev. A **96**, 053810 (2017).
[64] Y. H. Zhou, H. Z. Shen, and X. X. Yi, Phys. Rev. A **92**, 023838 (2015).
[65] H. Z. Shen, Y. H. Zhou, and X. X. Yi, Phys. Rev. A **91**, 063808 (2015).
[66] E. Togan, H.-T. Lim, S. Faelt, W. Wegscheider, and A. Imamoglu, Phys. Rev. Lett. **121**, 227402 (2018).
[67] I. Rosenberg, D. Liran, Y. Mazuz-Harpaz, K. West, L. Pfeiffer, and R. Rapaport, Sci. Adv. **4**, eaat8880 (2018).
[68] O. Kyriienko, I. A. Shelykh, and T. C. H. Liew, Phys. Rev. A **90**, 033807 (2014).
[69] G. Ramon, A. Mann, and E. Cohen, Phys. Rev. B **67**, 045323 (2003).
[70] R. Rapaport, R. Harel, E. Cohen, Arza Ron, E. Linder, and L. N. Pfeiffer, Phys. Rev. Lett. **84**, 1607 (2000).
[71] R. Rapaport, E. Cohen, A. Ron, E. Linder, and L. N. Pfeiffer, Phys. Rev. B **63**, 235310 (2001).
[72] S. De Liberato and C. Ciuti, Phys. Rev. B **77**, 155321 (2008).
[73] S. De Liberato and C. Ciuti, Phys. Rev. B **85**, 125302 (2012).
[74] S. De Liberato and C. Ciuti, Phys. Rev. Lett. **102**, 136403 (2009).
[75] M. Combescot and W. Pogosov, Eur. Phys. J. B **68**, 161 (2009).
[76] R. Ya. Kezerashvili and S. M. Tsiklauri, Few-Body Syst. **58**, 18 (2017).
[77] M. Szyniszewski, E. Mostaani, N. D. Drummond, and V. I. Fal'ko, Phys. Rev. B **95**, 081301(R) (2017).
[78] See Supplemental Material at http://link.aps.org/supplemental/10.1103/PhysRevLett.125.197402 for the details of derivation and additional analysis.
[79] V. Agranovich and B. Toschich, JETP **26**, 104 (1968), http://www.jetp.ac.ru/cgi-bin/dn/e_026_01_0104.pdf.
[80] T. Holstein and H. Primakoff, Phys. Rev. **58**, 1098 (1940).
[81] C. Emary and T. Brandes, Phys. Rev. Lett. **90**, 044101 (2003).
[82] C. Emary and T. Brandes, Phys. Rev. E **67**, 066203 (2003).
[83] F. P. Laussy, M. M. Glazov, A. Kavokin, D. M. Whittaker, and G. Malpuech, Phys. Rev. B **73**, 115343 (2006).
[84] E. del Valle Reboul, Quantum electrodynamics with quantum dots in microcavities, Ph. D. thesis, Madrid, 2009.
[85] I. G. Savenko, O. V. Kibis, and I. A. Shelykh, Phys. Rev. A **85**, 053818 (2012).
[86] M. Aßmann, F. Veit, J.-S. Tempel, T. Berstermann, H. Stolz, M. van der Poel, J. M. Hvam, and M. Bayer, Opt. Express **18**, 20229 (2010).
[87] S.-Y. Shiau, M. Combescot, and Y.-C. Chang, Phys. Rev. B **86**, 115210 (2012).
[88] M. Combescot and O. Betbeder-Matibet, Phys. Rev. B **80**, 205313 (2009).
[89] M. Combescot and J. Tribollet, Solid State Commun. **128**, 273 (2003).
[90] S.-Y. Shiau, M. Combescot, and Y.-C. Chang, Eur. Phys. Lett. **117**, 57001 (2017).
[91] H. Haug and S. W. Koch, *Quantum Theory of the Optical and Electronic Properties of Semiconductors* (World Scientific, Singapore, 1990).
[92] S. Larentis, H. C. P. Movva, B. Fallahazad, K. Kim, A. Behroozi, T. Taniguchi, K. Watanabe, S. K. Banerjee, and E. Tutuc, Phys. Rev. B **97**, 201407(R) (2018).
[93] The matrix element for an interband optical transition of a direct band-gap semiconductor can be estimated using the classical formula $2p_{cv}/m_0 \approx 20$ eV [see, e.g., A. A. Toropov and T. V. Shubina, *Plasmonic Effects in Metal-semiconductor Nanostructures* (Oxford University Press, Oxford, 2015)], which yields $g_0 = 0.052$ meV.
[94] E. W. Martin, J. Horng, H. G. Ruth, E. Paik, M.-H. Wentzel, H. Deng, and S. T. Cundiff, Phys. Rev. Applied **14**, 021002 (2020).
[95] B. Besga, C. Vaneph, J. Reichel, J. Estéve, A. Reinhard, J. Miguel-Sánchez, A. Imamoglu, and T. Volz, Phys. Rev. Applied **3**, 014008 (2015).
[96] S. Dufferwiel, Feng Li, A. A. P. Trichet, L. Giriunas, P. M. Walker, I. Farrer, D. A. Ritchie, J. M. Smith, M. S. Skolnick, and D. N. Krizhanovskii, Appl. Phys. Lett. **107**, 201106 (2015).